Hydrochemical Assessment of Groundwater Quality and Seawater Intrusion in the Coastal Aquifers of Limbe, Cameroon: Implications for Industrial Use

AZISE HELEN AYIMELE[1,2], MABEL NECHIA WANTIM[1], NCHINI LIVINUS[1], BIJINGSI MELISA[1], AKENJI VICTORINE[1,3], FANTONG WILSON Y.[3], AYONGHE SAMUEL N.[1]
[1]Department of Environmental Science
University of Buea
P.O. Box 63, Buea
CAMEROON
[2] Ministry of Water Resources and Energy
South West Regional Delegation
PMB 120, Limbe
CAMEROON
[3]Ministry of Scientific Research and Innovation
P.O. BOX 1457, Yaoundé
CAMEROON

Abstract: - The increasing dependence on groundwater in coastal urban settings such as Limbe, Cameroon, has raised concerns about seawater intrusion and its impact on water quality. This study investigates the hydro-chemical characteristics of groundwater at New Age found in an industrial estate in the Limbe II Municipality. This estate is located along the Atlantic coast where major industrial activities like the lone oil refinery in Cameroon is found. Twenty-five water samples were collected from November 2020 to May 2021 and assessed for their suitability for industrial use. Multifunctional pocket probes were used for in-situ measurements of temperature, pH, electrical conductivity, and total dissolved solids. Major ions were analyzed using ion chromatography (Metrohm 761 Compact IC), after passing samples through a 0.2 µm cellulose filter. Physicochemical parameters, including EC, TDS, and chloride (Cl^-) increased towards the coast, indicating progressive salinization. Ionic ratios: Na^+/Cl^- , Cl^-/HCO_3^- , SO_4^{2-}/Cl^- , Mg^{2+}/Ca^{2+} , Piper plots, and correlation matrices were employed to decipher the origin and extent of saline water mixing. Na–Cl facies, low Na^+/Cl^- (<0.86), and decreased SO_4^{2-}/Cl^- ratios in coastal wells pointed to incipient seawater intrusion, with well W6 showing the highest signs of impact. However, overall chloride concentrations remained below the 200 mg/L threshold indicative of intrusion onset. The correlation matrix revealed strong positive relationships among EC, TDS, major cations, and Cl^- , consistent with saline water sources. Total hardness varied widely (5–570 mg/L), with some samples (W6), producing very hard water that can affect industrial operations through corrosion or scaling. The findings confirm early-stage seawater intrusion in the shallow aquifers of Limbe, exacerbated by high groundwater abstraction, low elevation, and proximity to the ocean. A proactive groundwater management plan including pumping control and pretreatment of industrial water is recommended to preserve water quality and infrastructure integrity.

Key-words: - Seawater Intrusion, Groundwater Quality, Hydro-chemical Analysis, Limbe Coastal Aquifers, Industrial Water Suitability

1. Introduction

Coastal aquifers are exposed to severe seawater intrusion up to several kilometers inland **[1,2]**. Groundwater salinization is a pressing issue, largely resulting from unchecked and rapid groundwater exploitation to meet the growing freshwater demands of coastal regions, where over two-thirds of the world's population reside s **[3]**. As a result of excessive groundwater extraction from coastal aquifers the natural freshwater flow to the sea is disrupted, leading to a depression in the water table. Consequently, this allows seawater to migrate inland, ultimately contaminating nearby wells and compromising freshwater sources. Past studies recommend that appropriate setback distances must be imposed before pumping to ensure natural

filtration in subsoil, by means of soil aquifer treatment **[4-6]**. The inward movement of seawater results in the deterioration of groundwater quality., Seawater intrusion (SWI), therefore, a phenomenon triggered by excessive groundwater extraction, has emerged as a significant constraint on the sustainable use of groundwater resources in coastal regions. It is a pervasive issue that compromises water quality in coastal aquifers, pushing it beyond acceptable limits for drinking and irrigation **[7]**. Moreover, with global warming fueling ongoing sea level rise, these aquifers face an even greater threat, further jeopardizing future water supplies. Seawater intrusion into inland aquifers may be direct, but can also involve a range of complex geochemical processes like, inter-aquifer mixing, mobilization of brines, water-rock interaction and anthropogenic contamination **[8]**.

Limbe, a coastal city in Cameroon, is a hub for agro-industries, tourism and a deep seaport, hosting the country's sole oil refinery, SONARA. However, the city's rapid population growth, fueled by urban migration, has outstripped its water supply infrastructure, leading to significant challenges **[9]**. Moreover, CAMWATER, the public water supply company is unable to meet the ever-increasing water needs of the population, and only a few people can afford purified and treated bottled water **[10]**. The result is a high rate of groundwater exploitation via boreholes. More than 80% of residents in this area rely on groundwater for drinking, irrigation, commercial and industrial needs. Over 500 active boreholes now exist in the various localities that make up the coastal slopes of Mount Cameroon (Limbe) up from 27 in 2010 **[11]** that were found in the whole South West Region. Almost every household has a borehole for its water supply. However, there is a knowledge gap on the quality of water supplied by these boreholes as the water is hardly tested before use.

In recent times, there is an increasing focus on assessing seawater intrusion due to overexploitation of groundwater and rising sea levels **[12]**. Seawater intrusion phenomena have been reported with different degrees in almost all coastal aquifers around the globe.

Studies have deduced that excessive groundwater extraction can reduce groundwater gradients, allowing saline water to infiltrate and displace freshwater in the aquifer **[13]**. Moreover, excessive groundwater withdrawals have been reported to result not only in hydro-chemical changes of the water but also a drop in the water table level; reverse hydraulic gradient and consequently water quality deterioration in coastal areas **[14]**.

In the study area, excessive ground water abstraction is responsible for saline water intrusion **[15]**. Susceptibility to seawater intrusion is increased by low surface elevations, shallow depth-to-water levels, and proximity to the Atlantic shoreline **[9]**. The large number of functional water points currently existing and still growing at an exponential rate predisposes this area to overexploitation of the ground water resources, a phenomenon that equally leads to seawater intrusion. Irrigation, industrial infrastructure, potable water infrastructure as well as human health are all predisposed to the effects of the intruding seawater.

The suitability of groundwater for industrial applications is determined by factors such as chemical composition, hardness, and the presence of specific contaminants that can impact industrial processes **[16]**. Investigations have been conducted on the utilization of coastal groundwater resources for industrial purposes, considering the potential challenges posed by water quality issues and the need for appropriate treatment methods **[17]**. The integration of groundwater quality data into industrial water management strategies, including the implementation of water recycling and conservation measures, has been well documented **[18]**.

Existing studies in the area have explored water quality assessment using hydrochemistry and hydrogeological characteristics of the groundwater resources. Their findings revealed the presence of seawater intrusion in varying rates, as well as the influence of anthropogenic activities on groundwater quality thus providing valuable insights into the challenges faced by this community **[19,20,9,15]**. These researchers equally found out that ion exchange, simple dissolution of the country rock and proximity to the shoreline were controlling water quality in the study area.

The above studies and many other unpublished works have highlighted the challenges faced by coastal areas in managing groundwater resources sustainably. However, this study is more specific in that it was carried out at a company estate, in Limbola, within the industrial active zone close to the oil refinery. It employs hydro-geochemical techniques - including ionic trends, molar ratios, correlation matrices, and Piper Diagram analysis to assess seawater intrusion in the study area as well as the suitability of this water for industrial installations and uses. By synthesizing the findings of previous studies and conducting additional

research in the study area; like detailed mapping of the aquifer, numerical modelling of groundwater flow to simulate SWI and predict future trends, etc., policy makers and water resource managers can develop strategies to mitigate the impacts of seawater intrusion and ensure the availability of quality groundwater for various uses.

2. Materials and Methods

2.1 Study site

The study area is the New Age property found in Limbola, in Limbe II Municipality which is approximately 10 m above sea level (Fig. 1). Limbe II stands out as the economic heartbeat of the city if not of the South West Region as a whole as it plays host to 03 major corporations: The National Oil Refinery (SONARA), the Cameroon Development Corporation (CDC), and the Shipyard (Chantier Naval), taken over by New Age. In addition to these is the multiplicity of tourists, leisure and accommodation sites (like the many beaches spread along the Atlantic coast, Mount Cameroon National Park, hotels, etc.). Limbe II has an approximate population of about 100,000 people **[21].** It receives many visitors and rural–urban migration makes it one of the fastest growing areas in the South West Region. This in turn causes problems typical to tropical megacities, like sluggish infrastructural growth, pollution, poor access to basic needs like water, sanitation and hygiene.

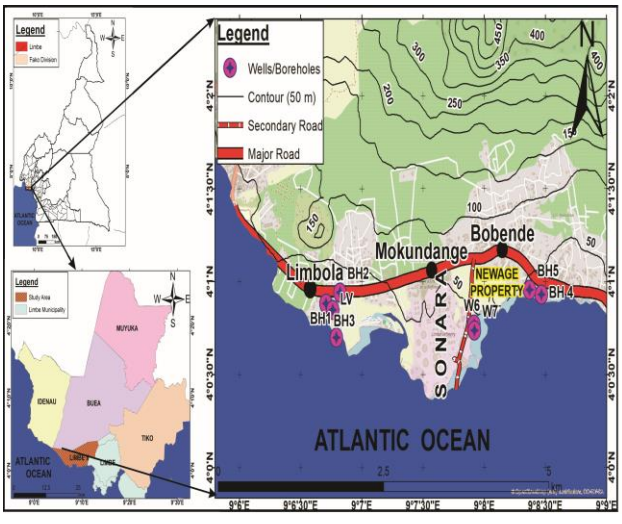

Fig. 1: Map of the Study Area and Location of the monitoring wells and proximal boreholes

The high demographic and economic development activities taking place in this area equally occur along with environmental destruction that also includes deterioration of the groundwater quality.

2.2. Methodology

Geophysical techniques were used to identify potential points at the New Age Property from where two shallow wells were dug to add to an already existing hand-dug well that has been a main water source in a neighborhood in Limbola. These served as monitoring wells for the period of the study. Seven sets of data were thus collected from the three hand-dug wells to monitor for sea water intrusion in this area. Sampling for physico-chemical parameters from the monitoring wells was done for a period of seven months from November, 2020 to May, 2021. The last samples in the month of May from five boreholes identified to be in close proximity to the ocean, just like the monitoring wells, served mainly for control. A total of twenty-five (25) water samples were collected from the monitoring wells (Fig. 1) during the seven months period and taken to the laboratory for analysis. All water samples were collected in pre-conditioned high-density polyethylene (HDPE) bottles. These sampling bottles underwent a rigorous cleaning process to ensure they were contaminant-free. Initially, they were washed with detergent, followed by a 10% nitric acid rinse. They were finally rinsed twice with distilled water to guarantee their purity. Sampling procedures were carried out as described by **[22]**. During sampling, a bucket tied to a rope was dropped in to the well to collect the water which was transferred to the sampling bottles after checking physical parameters (Temperature, pH, EC, TDS).

Similar procedures were employed for the sampling of the boreholes but for the fact that these were pumped for 5 minutes before sample collection. Each sample bottle was provided with an identification label on which the following information was legibly and indelibly written: sample code, date and time of collection, pH, Temperature and EC. In the field, all water samples were tightly capped and preserved in a cooler packed with ice block to maintain a suitable temperature of about 4 ^{o}C, before transporting to the laboratory.

2.2.1. In-situ field measurements

Parameters that control interaction of inorganic constituents in groundwater which are usually measured in-situ in the field are: Temperature, pH, Electrical Conductivity (EC), and Total Dissolved Solids (TDS). Each of these parameters was measured on the field by immersing pre-calibrated probes in to the water in the collector.

Temperature was measured as close to in-situ conditions as possible. The pH controls most of the

organic and inorganic constituents in groundwater. In this study the pH and temperature were measured using the Pocket pH Tester probe (HYDROLITE HL101) which has an accuracy of ±0.002 pH units. Electrical Conductivity (EC) provides a rough idea of the total dissolved solids. All EC values for this study were recorded in μScm^{-1}. A complex multifunctional pocket EC Tester (HYDROLITE HL102) was used for measurement of conductivity, TDS, and salinity. This equipment has an accuracy of ±1%F.S.

2.2.2. Laboratory Analyses

Laboratory analysis was carried out at the Institute of Geological and Mining Research in Nkolbisson, Yaounde. Major ion concentrations were determined using ion chromatography (Metrohm 761 Compact IC). A known standard was run after every five samples to maintain the analytical precision. All samples were filtered through a 0.2 µm cellulose filter prior to major ions determination. This was to prevent blockage of the IC analytical column. The reproducibility of the analytical procedures was checked by carrying out duplicate analysis. Alkalinity was measured by titration with HCl. Total water hardness (TH) was measured by summing the concentrations of the multivalent cations Ca^{2+} and Mg^{2+} in the samples **[23]**.

2.3 Data analyses

Analytical precision for cations (Na^+, K^+, Mg^{2+}, and Ca^{2+}) and anions (F^-, Cl^-, NO_3^- , SO_4^{2-} , and HCO_3^-) was checked using ionic balance error (IBE) **[24],** following equation (1) below.

$$IBE = \frac{\sum Cations - \sum \text{Anions}}{\sum Cations + \sum Anions} x\ 100 \qquad (1)$$

An error of ±5% is acceptable, while beyond this accuracy, the analytical result is doubtful **[25]**. In this study, the charge balances for the major ions were within the limit ±0.24 % for all samples. The data sets were thus selected for further analysis. Correlation analysis was carried out for hydrogeochemical characteristics of analyzed water samples and the significance of correlation coefficients were tested using the statistical software, SPSS version 21. ArcGIS version 10.1, a geographic information system (GIS) software package, was used to create various maps.

To fully understand the relationship between the geology of the area and the hydro-geochemistry of the groundwater, hydrogeochemical tools were used. Ionic ratios for indicative elements are useful hydrogeochemical tool to identify source rock of ions and formation contribution to solute hydro geochemistry **[26]**. The piper trilinear diagram was created using GW-Chart v.1.29.0 and it was employed to reveal geochemical types of the groundwater and understand the seawater intrusion processes in the area **[27,28]**.

3. Results and Discussion

A total of 20 groundwater samples from 3 shallow wells plus an additional 5 samples from boreholes (deep wells) were analyzed for 16 constituents including the major anions and cations as shown in Tables 1 & 2.

3.1 Physico-chemical Trends

Electrical conductivity (EC), TDS and Cl^- increased from the inland to the coastal wells. The inland well (LV) was about 8 m deep and about 50 m from the shore. LV had a mean EC of 152 µS/cm showing a moderate decrease from 233 µS/cm (Nov) to 130 µS/cm (April) and TDS decreased from 156 mg/L to 85 mg/L giving a mean of 99 mg/L (Fig. 2 and Fig. 3A). Alkalinity peaked at 3147 mg/L (Dec) and dropped drastically to 22 mg/L in April. W6 is 6 m deep and is closest to the Ocean (20 m from the Ocean). This well had an average EC of 450 µS/cm (peaking at 848 µS/cm in April) and TDS ranged from 89 mg/L to 559 mg/L with a mean of 362 mg/L (Fig. 2 and Fig. 3B). Alkalinity experienced a decrease from 771 mg/L to 77 mg/L. W7 is 4 m deep and about 30 m from the shore. For this well, EC increased from 355 µS/cm (Dec) to 510 µS/cm (Apr) with a mean of 430 µS/cm; while TDS ranged from 235 mg/L to 338 mg/L with an average of 282 mg/L (Fig. 2 and Fig. 3C). Alkalinity, just like in W6, also experienced a decrease from 854 mg/L to 103 mg/L. Salinity mirrored EC with a progressive average increase from LV (0.07ppt) to W7 (0.21 ppt) to W6 (0.26 ppt) in the monitoring wells while all pH values were near neutral (6.9–7.6), and stayed within the WHO recommended range (6.5–8.5) for drinking water.

Following the physical water properties, the deep boreholes in contrast to the monitoring wells, remained fresh with mean EC=175 µS/cm and TDS=118.8 mg/L (Fig. 2).

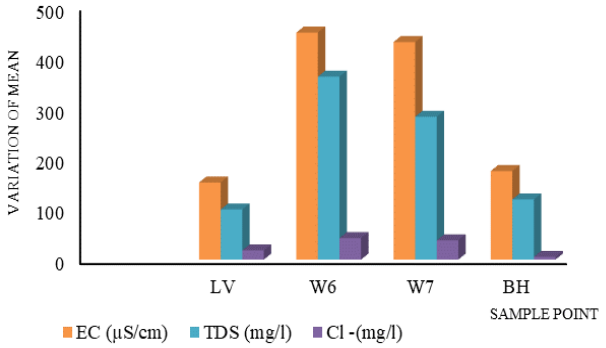

Fig. 2: Variation of mean EC, TDS and Cl at the sampling points LV, W6, W7 and the boreholes

Seasonally, total salinity (that is, EC, TDS, salinity ppt) increased from inland to the coast (LV < W7 < W6). Well, LV is furthest inland and thus little mineralization as opposed to W7 which is furthest to the coast. Thus, well, W6 showed the highest mean EC (450 µS/cm) and TDS (361.6 mg/L), peaking in April (848 µS/cm) which is the dry season (Fig. 3B). Well, W7 (intermediate) registered lower mean EC (430.1 µS/cm) values compared to W6 (Fig. 2). The Inland well LV, remained relatively fresh (mean EC=152 µS/cm) while all the five boreholes were much fresher (mean EC=175 µS/cm) (Fig. 2).

The dominant anion in W6 was Chloride (Cl^-) which jumped from 6.9 mg/L peaking at 180 mg/L (Dec) and then to 33.4 mg/L (April). The high measurement registered in December was likely due to episodic tidal intrusion during season transition.

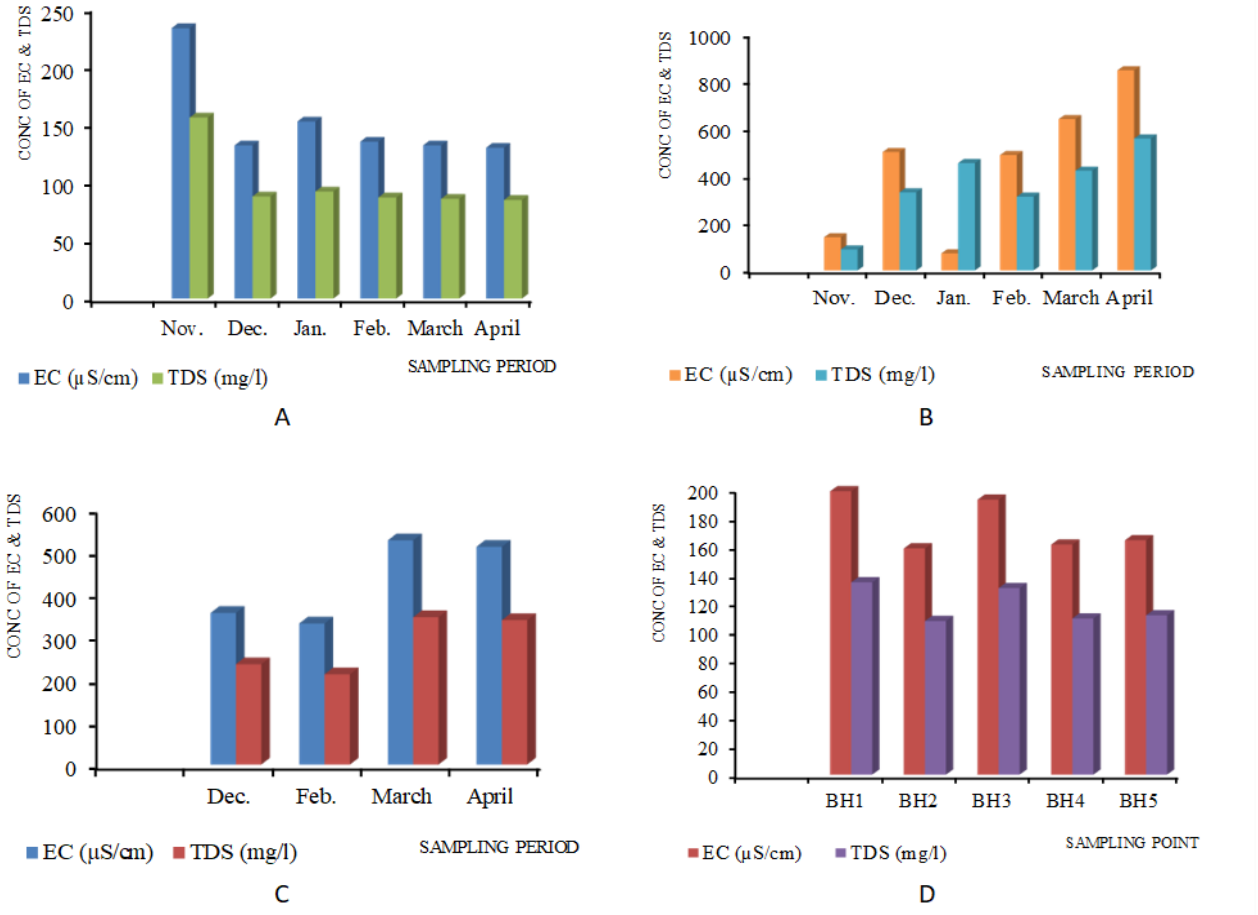

Fig. 3: Comparative plots of EC and TDS in the sampling points. A: at LV; B: at W6; C at W7 and D at the boreholes

The dominant cation, sodium (Na^+) rose from 1.3 mg/L to 77.3 mg/L (Fig.4). Magnesium (Mg^{2+}) and calcium (Ca^{2+}) also rose from 0.74mg/L to 10.9 mg/L and 14.8mg/L to 21.2 mg/L respectively (Fig.4). This is consistent with a Na–Cl facies evolving over time. Potassium (K^+) and sulfate (SO_4^{2-}) increased but just to a lesser extent (Table 1).

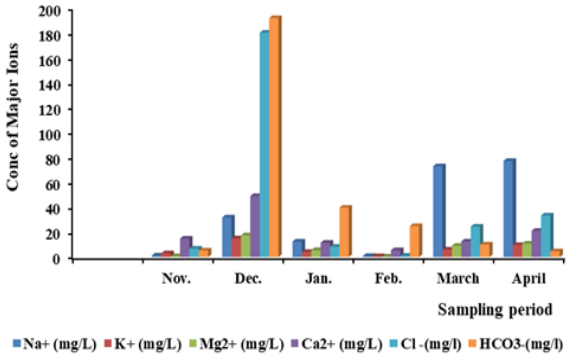

Fig. 4: Monthly variation of major ions at W6

The dominant anion in W7 was also chloride (Cl^-) which decreased from 88.9 mg/L to 18.9 mg/L. The dominant cation, Na^+ varied around 60 mg/L to 82 mg/L (Fig. 5), while Mg^{2+} and Ca^{2+} tracked the EC/TDS increases (Table 1), indicating seawater freshwater mixing.

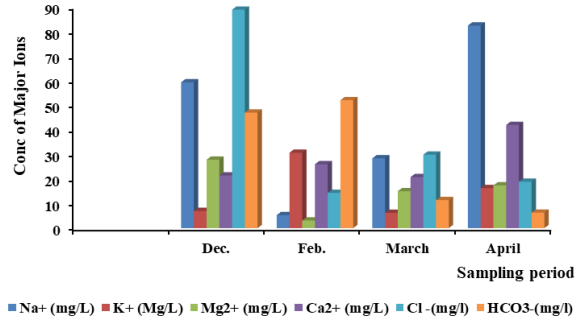

Fig. 5: Monthly variation of major ions at W7

The dominant ions in LV were Ca^{2+} and HCO_3^-. Calcium (Ca^{2+}) ranged from 9 mg/L to 36 mg/L while Na^+ ranged from 0.5 mg/L to a peak value of 90.47 mg/L in April (Fig. 6). HCO_3^- rose from 5 mg/L to 46 mg/L. Unlike the other wells, chloride (Cl^-) stayed low (11 mg/L to 37 mg/L) with no clear upward trend. The Ca–HCO_3 water type was the dominating facies in this well. These results strongly reveal that though most parameters remained within the WHO limit, (except for high TDS in the W6 April sample) there is a gradual increase of seawater precursors and hence a clear salinity gradient towards the coast.

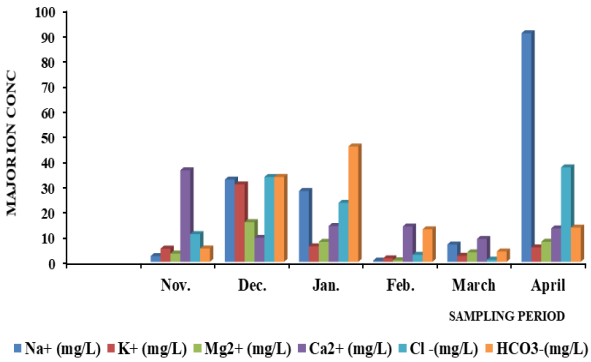

Fig. 6: Monthly variation of major ions at LV

The observed gradients and ratios suggest incipient seawater intrusion in the New Age Limbe aquifer.

The increase in conductivity and chloride towards the coast indicates saltwater mixing. The highest-salinity samples (W6 in April: EC 848 µS/cm, Cl^- 33.4 mg/L) still have Cl^- values far below the 200 mg/L threshold proposed for intrusion onset, however, the trend is evident. The World Health Organization **[29]** states that drinking water usually tastes salty above 250 mg/L of Cl^-, so current levels are acceptable.

The observed spatial trend of increasing EC, TDS, and Cl^- (Fig. 3) in the monitoring wells towards the shoreline underscores the vulnerability of shallow aquifers under high abstraction pressure as is the case with the study area. Moreover, groundwater in the area just like other coastal parts of Limbe is recharged from the Mount Cameroon area **[9]** which flows down slope into the low-lying shoreline where some areas are below sea level (b.s.l). Thus, during the rainy season sea levels increase at high tide and the land is submerged by the sea. This leads to seawater intruding the aquifer formations in the low-lying areas. The strong correlation between Cl^- and EC (R^2=0.86) in coastal samples confirms that salinity is driven largely by chloride (sea salt) rather than other ions. Although existing boreholes (BH1–BH5) exhibit lower salinity than monitoring wells, which is likely due to greater depth and slower response, continued pumping could propagate the saline interface. Groundwater management via controlled pumping rates, artificial recharge, and buffer- zone setbacks is recommended **[4,5]**.

Table 1: Statistical analysis of hydro-chemical parameters measured for the 6-month monitoring at three shallow wells

Month	Sample	Temp (°C)	pH	EC (S/cm)	Sal (ppt)	TDS (mg/l)	Alc (mg/l)	Na^+ (mg/l)	K^+ (mg/l)	Mg^{2+} (mg/l)	Ca^{2+} (mg/l)	Cl^- (mg/l)	F^- (mg/l)	NO_3^- (mg/l)	HCO_3^- (mg/l)	SO_4^{2-} (mg/l)	TH (mg/l)
Nov.	**W6**	27.4	7.13	140.6	0.06	89.09	88.02	1.33	3.07	0.74	14.82	6.89	0.03	5.85	5.37	6.17	40.051
Dec.	**W6**	24.1	7.61	502	0.25	331	771	31.89	15.09	17.53	49.08	180.23	0.63	0	191.97	1.95	194.689
Jan.	**W6**	27	7.11	72.5	0.34	455	651	12.55	4.24	5.69	11.59	8.38	0.08	0	39.71	3.21	52.355
Feb.	**W6**	25.9	7.31	489	0.23	312.65	409	0.93	0.77	0.37	5.56	1.06	0.03	0.39	24.95	0.33	15.406
March	**W6**	24.5	6.88	641	0.31	423	167	73.03	6.11	9.18	12.62	24.51	0.2	2.5	10.19	9.63	69.288
April	**W6**	24.4	7.28	848	0.42	559	77	77.32	9.79	10.89	21.2	33.42	0.02	2.08	4.7	24.35	97.740
Mean		25.55	7.22	448.85	0.27	361.62	360.50	32.84	6.51	7.40	19.15	42.42	0.17	1.80	46.15	7.61	78.26
Std		1.427	0.245	295.749	0.123	160.658	299.103	34.691	5.186	6.552	15.513	68.593	0.238	2.256	72.703	8.841	63.400
Min		24.1	6.88	72.5	0.06	89.09	77	0.93	0.77	0.37	5.56	1.06	0.02	0	4.7	0.33	15.406
Max		27.4	7.61	848	0.42	559	771	77.32	15.09	17.53	49.08	180.23	0.63	5.85	191.97	24.35	194.689

Month	Sample	Temp (°C)	pH	EC (S/cm)	Sal (ppt)	TDS (mg/l)	Alc (mg/l)	Na^+ (mg/l)	K^+ (mg/l)	Mg^{2+} (mg/l)	Ca^{2+} (mg/l)	Cl^- (mg/l)	F^- (mg/l)	NO_3^- (mg/l)	HCO_3^- (mg/l)	SO_4^{2-} (mg/l)	TH (mg/l)
Dec.	**W7**	24	7.29	355	0.17	235	551	59.36	7	27.84	21.41	88.93	0.17	0	47.03	9.08	168.022
Feb.	**W7**	25.8	7.2	330.3	0.15	211.25	854	5.29	30.69	3.1	26.01	14.35	0.1	25.4	52.09	57.63	77.704
March	**W7**	24.4	7,28	525	0.26	345	187	28.42	6.23	15.04	20.77	29.89	0.08	0.24	11.41	6.3	113.752
April	**W7**	24.3	7.01	510	0.25	338	103	82.48	16.31	17.39	42.01	18.88	0.46	2.11	6.28	13.05	176.459
Min		24	7.01	330.3	0.15	211.25	103	5.29	6.23	3.1	20.77	14.35	0.08	0	6.28	6.3	77.704
Max		25.8	7.29	525	0.26	345	854	82.48	30.69	27.84	42.01	88.93	0.46	25.4	52.09	57.63	176.459
Mean		24.63	7.17	430.08	0.21	282.31	423.75	43.89	15.06	15.84	27.55	38.01	0.20	6.94	29.20	21.52	133.98
Std		0.80	3.59	101.64	0.06	69.09	346.53	33.95	11.38	10.15	9.92	34.57	0.18	12.34	23.69	24.24	40.434

Month	Sample	Temp (°C)	pH	EC (S/cm)	Sal (ppt)	TDS (mg/l)	Alc (mg/l)	Na^+ (mg/l)	K^+ (mg/l)	Mg^{2+} (mg/l)	Ca^{2+} (mg/l)	Cl^- (mg/l)	F^- (mg/l)	NO_3^- (mg/l)	HCO_3^- (mg/l)	SO_4^{2-} (mg/l)	TH (mg/l)
Nov.	**LV**	27.3	7.67	233	0.1	156	86.73	2.29	5.22	3.27	36.25	10.98	0.04	10.94	5.29	21.26	103.972
Dec.	**LV**	24	8.41	132	0.06	88	3147	32.55	30.63	15.69	9.48	33.56	0.04	0	33.61	24.73	88.236
Jan.	**LV**	27.2	6.89	152.6	0.07	92.25	748.5	28.06	6.145	7.905	14.165	23.33	0.1	0	45.66	14.96	67.899

Feb.	**LV**	25.7	6.84	135.2	0.06	87.1	211	0.5	1.38	0.63	13.98	2.78	0.01	6.85	12.87	13.58	37.501
March	**LV**	24.6	7.08	132	0.06	86	67	6.86	2.38	3.74	9.06	0.87	0.26	0.03	4.09	0.55	38.013
April	**LV**	24.4	7	130	0.06	85	22	90.47	5.71	7.94	13.21	37.36	0.39	0.97	13.54	17.91	65.658
Min		24	6.84	130	0.06	85	22	0.5	1.38	0.63	9.06	0.87	0.01	0	4.09	0.55	37.501
Max		27.3	8.41	233	0.1	156	3147	90.47	30.63	15.69	36.25	37.36	0.39	10.94	45.66	24.73	103.972
Mean		25.53	7.32	152.47	0.07	99.06	713.71	26.79	8.58	6.53	16.02	18.15	0.14	3.13	19.18	15.50	66.880
Std		1.445	0.614	40.314	0.016	28.008	1221.853	33.996	10.972	5.310	10.158	15.618	0.152	4.663	16.743	8.386	26.574

NOTE: TDS=Total Dissolved Solid; EC=Electrical Conductivity; Alc=Alkalinity; Sal= Salinity; TH=Total Hardness; Min=Minimum; max=Maximum; Std= standard Deviation

Table 2: Statistical analysis of the boreholes collected in May

	Sample	**Temp (°C)**	**pH**	**EC (S/cm)**	**Sal (ppt)**	**TDS (mg/l)**	**Alc (µeq/l)**	**Na^+ (mg/l)**	**K^+ (mg/l)**	**Mg^{2+} (mg/l)**	**Ca^{2+} (mg/l)**	**Cl^- (mg/l)**	**F^- (mg/l)**	**NO_3^- (mg/l)**	**HCO_3^- (mg/l)**	**SO_4^{2-} (mg/l)**	**TH (mg/l)**
May	**BH1**	23.9	6.69	198.5	0	134.7	0	14.96	5.89	8.03	14.21	1.42	0.08	2.73	6.31	1.83	30.53516
	BH2	23.6	6.3	158.5	0	107.6	0	11.29	4.34	5.69	7.98	14.42	0.04	7.47	2.53	4.42	21.44769
	BH3	23.7	6.38	192.6	0	130.7	0	12.6	2.54	6.34	10.38	5.16	0.09	21.59	4.53	3.12	26.43159
	BH4	23.8	6.2	161.2	0	109.4	0	10.51	3.72	5.53	11.13	4.2	0.05	20.53	3.57	3.55	23.5549
	BH5	23.6	6.89	164.2	0	111.6	0	12.08	4.79	6.22	9.6	1.26	0.06	1.99	6.46	1.5	30.3284
Min		23.6	6.2	158.5	0	107.6	0	10.51	2.54	5.53	7.98	1.26	0.04	1.99	2.53	1.5	21.44769
Max		23.9	6.89	198.5	0	134.7	0	14.96	5.89	8.03	14.21	14.42	0.09	21.59	6.46	4.42	30.53516
Mean		23.72	6.492	175	0	118.8	0	12.288	4.256	6.362	10.66	5.292	0.064	10.86	4.68	2.88	26.46
Std		0.130	0.288	18.982	0.000	12.846	0.000	1.691	1.244	0.993	2.303	5.380	0.021	9.551	1.710	1.213	4.035

3.2 Hydro-chemical Facies

Sodium and calcium were the dominant cations ($Na^+ > Ca^{2+} > Mg^{2+} > K^+$) and chloride dominated among anions ($Cl^- > SO_4^{2-} > HCO_3^- > NO_3^-$) – a pattern typical of coastal aquifers influenced by seawater. These facies are consistent with published coastal-groundwater studies that attribute high Na^+ and Cl^- to seawater mixing **[30]**. The Piper's trilinear plot revealed four main types of water as follows: Na–Cl saline water type, Ca–Cl, Ca–Na–HCO_3^- mixed water type and Ca–HCO_3^- freshwater type in the wells (Fig. 7a). The boreholes exhibited three major types, Ca–Cl, Ca–Na–HCO_3^- and Ca–HCO_3 (Fig. 7b). The samples from W6 show Na-Cl type, which generally indicates a strong seawater influence **[31]** or up-coming of deep saltwater as may be the case with the April sample from LV (dry season sample) which had the Na–Cl water type. This water type is probably a result of significant seawater intrusion. Most boreholes and some four samples from LV (Feb), W6 (Dec) and W7 exhibited Ca–Cl water type indicating salinization which likely resulted from mixing with seawater and cation exchange reactions **[32]**. The variation in the cationic concentrations where Na^+ has high concentrations as compared to Ca^{2+} and Mg^{2+} in some locations can result from saline water intrusion **[33]**.

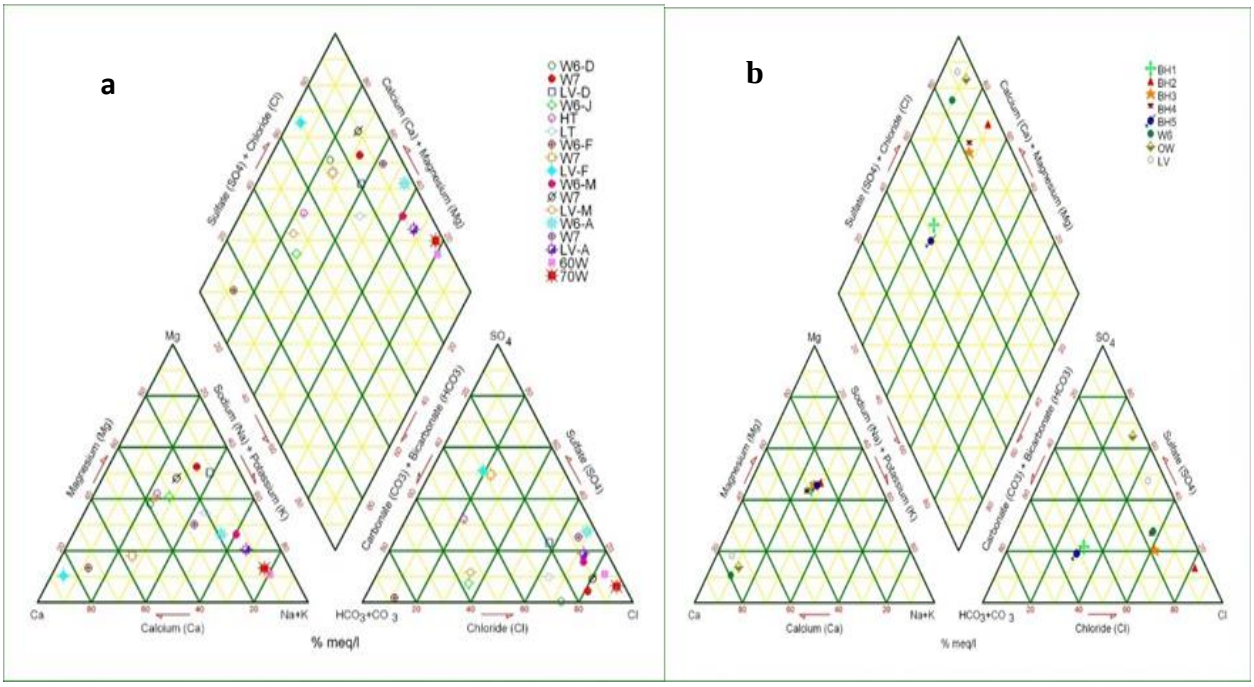

Fig. 7: Piper Diagram showing a) the hydro-chemical composition in the monitoring wells, LV, W6 and W7 and b) the hydro-chemical composition of the water in the borehole sample

3.3 Seawater indicators

According to **[34]**, seawater typically has sodium and chloride as its dominant ions, whereas freshwater is characterized by calcium and bicarbonate ions. Therefore, high levels of Na^+ and Cl^- ions in coastal ground water may be an indication of significant effects of seawater mixing and the occurrence of saline water **[35]**. Elevated amounts and correlations between EC, TDS, Cl^- and major ions are equally good indicators of saline intrusion in groundwater. Ionic ratios of Na^+/Cl^-, SO_4^{2-}/Cl^-, $Mg^{2+}/Ca^{2+}$and Cl^-/HCO_3^- exhibit characteristic threshold values beyond which seawater signals are indicative of their influence on groundwater.

3.3.1 Ionic Ratios

Ionic relationships are crucial for defining the origin of solutes and the various processes that form groundwater chemical composition. Na/Cl ionic ratio

has been widely used to evaluate the effect of seawater encroachment in an aquifer **[36,37]**. Na/Cl ratios lower than the theoretical seawater value of 0.86 indicate seawater encroachment **[35]**. This means that fresh groundwater has become polluted by the seawater exchanger **[38-40]**, hence inverse cation exchange takes place and Na^+ is taken up by the exchanger.

In the present study, molar ratios in the shallow monitoring wells reflected mixed fresh and marine signatures. Na^+/Cl^- ranged from 0.27–11.82 at the inland point (LV) with 33.33% of the samples having values less than the seawater ratio of 0.86. The coastal point W6 had Na/Cl values ranging from 0.27 to 4.47 and still 33.33% had values below 0.86 while W7 ranged from 0.55 to 6.55 with 25% values below the 0.86 seawater value. A Na/Cl ratio approximating unity suggests that Na^+ and Cl^- ions likely originate from the dissolution of evaporites [**41-43]**. In pure seawater, where Na/Cl molar ratio is approximately 0.86, intrusion drives Na/Cl towards that value and a ratio of less than 0.86 indicates the case of certain pollutions and obviously indicates seawater influence **[44]**. A Na/Cl molar ratio greater than 1 means that silicate weathering may be contributing to Na^+ ions in the groundwater **[42]**. For this study most of the shallow wells had Na/Cl >0.86, reflecting dominance of freshwater or other Na^+ sources inland **[45,35]**. However, a few samples (minima 0.27–0.55 in LV–W7) fell well below 0.86, signifying localized saltwater mixing. In the deep boreholes the Na/Cl molar ratio ranged from 1.7–15.8 clearly reflecting Na-enrichment (from rock weathering or cation exchange) with little marine signature. Therefore, only some shallow samples meet the <0.86 intrusion criterion, consistent with early-stage intrusion in parts of the aquifer. These findings are in line with the observations of **[9,15]**.

A high Cl^-/HCO_3^- ratio is a key and sensitive salinization indicator known as the Simpson's ratio **[46]**. Todd (2004) **[47]** classified the ratio Cl^-/HCO_3^- : **<0.5** as unaffected, **0.6–6.6** moderately affected, and **>6.6** strongly intruded. The Cl^-/HCO_3^- results from the shallow wells averaged 2–3.5 and ranged from 0.08–12.6. These mean values lie in the moderately salinized category. Well W7 (mean 3.5) had higher Cl^-/HCO_3^- value than inland LV (2.0), reflecting chloride enrichment from seawater. None of the well samples (total samples per well) consistently exceeded the strong-intrusion cutoff (>6.6) on average, though a few individual monthly measures like W6 (April: Cl^-/HCO_3^- =12.6) did. Thus, the Cl/HCO_3 indicator corroborates mild to moderate seawater mixing near the coast.

Mg^{2+}/Ca^{2+} (or Ca^{2+}/Mg^{2+}) ratio: Seawater has much higher Mg^{2+} relative to Ca^{2+} (mol ratio = 5, Ca/Mg = 0.2), whereas typical limestone aquifers have Ca/Mg >1. Intrusion tends to drive Mg/Ca upward and Ca/Mg downward. The shallow wells had Mg/Ca mean range from 0.61–1.05 (equivalently Ca/Mg ranged from 0.95–1.64). These are near unity, much higher Ca/Mg (lower Mg/Ca) than seawater. About 25% of samples in this study had Mg/Ca ratio above 1, suggesting possible seawater signal. According to **[48]**, samples with Ca/Mg approaching seawater values (very low) indicate intrusion. In this study, Ca/Mg (0.95–1.6) remains well above the approximately 0.2 value of seawater, implying that fresh-water sources and rock weathering still dominate. In the deep boreholes, Mg/Ca ranged from 0.82–1.18, reflecting fresher, Ca-rich water. Thus Mg/Ca ratios suggest limited seawater mixing.

SO_4^{2-}/Cl^- ratio: Seawater intrusion often lowers SO_4^{2-}/Cl^- because ocean water has relatively less sulfate (much is precipitated as gypsum). In the present study, W6 (coastal) had a very low SO_4^{2-}/Cl^- mean (0.16), whereas inland LV was 0.56. Low ratios (especially <0.2) are characteristic of seawater-influenced zones. Recent studies noted that low SO_4^{2-}/Cl^- highlights saltwater–freshwater mixing through predominance of Cl^- over SO_4^{2-} **[38]**. The boreholes data in this study showed higher SO_4^{2-}/Cl^- values, again reflecting fresher chemistry. In summary, the depressed SO_4^{2-}/Cl^- in near-coast wells supports a marine component, consistent with the other evidence.

3.3.2 Hydro-chemical Correlation matrix

The correlation between Cl and EC has been used worldwide to highlight the effect of seawater intrusion, whereby simultaneously high values of Cl and EC indicate the most affected by the marine intrusion effect **[49,50]**. Strong positive correlation between EC and TDS with ions of Na, Cl and HCO_3 and other major ions reflect the influence of these ions to increase the EC and TDS values. A positive correlation between Cl and Na emphasis the effects of chemical weathering. It also indicates sea water intrusion influence and secondary leaching of salts **[51-53]**. In this study, the correlation matrix showed a tight cluster of electrical conductivity (EC),

TDS, salinity, Na^+ , K^+ , Mg^{2+} , Ca^{2+} , Cl^- and SO_4^{2-} (EC-Na: r=0.999, EC–K: r=0.993, EC–Mg: r=0.950, EC–Ca: r=0.967, EC–Cl: r=0.861, EC–SO_4 : r=0.522) (Table 3). This type of high and uniform correlations indicates a common saline source, which is consistent with seawater mixing. This is also an indication that they are dedicated to essential geochemical methods through mineralogical impact **[54]**. In coastal aquifers, EC and Cl^- typically rise together as seawater intrudes; indeed, high EC, Na, K, Mg, Cl and SO_4 are hallmark "saltwater" signatures **[55]**. Generally, chloride (Cl^- > 200 mg/L) and EC (EC > 1000 µS/cm) are noted as the simplest intrusion indicators and usually reflect seawater influence **[56]**. Though the present study shows lower values for these parameters, their proportional co-variation is very clear. The near 1.00 correlations among Na, K, Mg, and Ca (with r range = 0.95–0.99) suggest mixing rather than isolated sources. Saltwater is rich in Na–Cl and contains appreciable Mg, Ca and K; the matrix thus implies that all these ions rise and fall together (freshwater dilution vs. saline incursion). The correlation between Na^+/SO_4^{2-} (r = 0.61) reflect their common origin, that is, coming from former times, reflecting a long residence time. Cation exchange and mineral reactions are the geochemical processes that can further shape these trends. Generally, when seawater mixes with freshwater it often triggers Na–Ca (and Na–Mg) ion exchange on clays: incoming Na^+ from seawater can displace Ca^{2+} and Mg^{2+} on aquifer materials, sometimes elevating Ca and Mg in water beyond conservative mixing **[57]**. In this correlation matrix (Table 3), all cation pairs correlate positively (e.g. Ca–Na r=0.966, Mg–Na r= 0.957, Ca–Mg r=0.952), suggesting that exchange effects may be small compared to bulk mixing. However, the fact that the water types are Ca-Cl, Na-Cl and Ca/Mg-Mix **[57]** implies some cation exchange is occurring in the mixing zone. In the study area; silicate weathering is the major source that releases ions into groundwater by the processes of ion-exchange; simple dissolution of the country rock, characteristic of groundwater in basaltic terrains, and reverse ion exchange which is common in coastal regions with seawater intrusion **[9]**. Nutrients and certain minor ions in the matrix suggest human impacts. Nitrate (NO_3^-) is negatively correlated with the salinity cluster (NO_3^-–EC r= –0.15, NO_3^-–Cl^- r= –0.26, NO_3^-–Na^+ r= –0.17). NO_3^- thus rises where salts are low and this is typical of land-derived contamination, probably from agricultural or sewage sources. Intensive agricultural activities with constant use of farm inputs are very common in the study area. Irrigation with N-fertilizers and domestic sewage are known to elevate NO_3^- in coastal aquifers **[56]**.

Table 3: Correlation matrix of the major physico-chemical parameter

	Temp (°C)	pH	EC (µS/cm)	TDS (mg/l)	Sal (ppt)	Alc (µeq/l)	Na+ (mg/l)	K+ (mg/l)	Mg2+ (mg/l)	Ca2+ (mg/l)	Cl - (mg/l)	F - (mg/l)	NO3- (mg/l)	HCO3- (mg/l)	PO43- (mg/l)	SO42- (mg/l)
Temp (°C)	1															
pH	0.035	1														
EC (µS/cm)	-0.159	0.587	1													
TDS (mg/l)	-0.157	0.588	1.000	1												
Sal (ppt)	-0.155	0.589	1.000	1.000	1											
Alc (µeq/l)	0.003	0.606	0.069	0.070	0.071	1										
Na+ (mg/l)	-0.177	0.589	0.999	0.999	0.999	0.074	1									
K+ (mg/l)	-0.166	0.616	0.993	0.993	0.993	0.113	0.992	1								
Mg2+ (mg/l)	-0.286	0.640	0.950	0.950	0.950	0.155	0.957	0.962	1							
Ca2+ (mg/l)	-0.122	0.634	0.967	0.966	0.966	0.054	0.966	0.972	0.952	1						
Cl - (mg/l)	-0.244	0.660	0.861	0.861	0.861	0.174	0.866	0.880	0.931	0.914	1					
F - (mg/l)	-0.283	0.383	0.565	0.565	0.565	0.040	0.583	0.529	0.573	0.612	0.635	1				
NO3- (mg/l)	-0.013	-0.400	-0.151	-0.153	-0.154	-0.196	-0.169	-0.138	-0.247	-0.138	-0.260	-0.268	1			
HCO3- (mg/l)	-0.011	0.334	0.067	0.068	0.069	0.356	0.068	0.085	0.169	0.187	0.465	0.478	-0.183	1		
PO43- (mg/l)	0.015	0.351	0.337	0.336	0.336	-0.174	0.356	0.336	0.324	0.388	0.292	0.251	-0.082	-0.191	1	
SO42- (mg/l)	0.239	0.467	0.522	0.520	0.521	0.243	0.517	0.534	0.442	0.565	0.396	0.248	0.217	0.012	0.261	1

Note: Highlighted areas indicate points of high correlation

In essence, the matrix suggests freshwater-seawater mixing with some evidence of clay-cation exchange. The EC–TDS–major-ion correlation cluster strongly points to progressive salinization from the sea **[55,56]**; while the classic geochemical effect of intrusion; Na^+ replacing Ca^{2+} on exchange sites **[57]**, is consistent with the predominance of Na–Cl facies. The anti-correlation of NO_3^- with the seawater indicators points to anthropogenic nutrient input in fresher groundwater. High NO_3^-, in particular, is a classic sign of land-derived pollution, as noted in coastal studies.

3.4 Industrial Suitability

Evaluation of the suitability of groundwater for industrial use was based on water quality standards of TDS, Na and Cl, and their potential impacts on industrial processes. TDS in wells LV (mean 362 mg/L) and W6 (mean 282 mg/L) approached the soft- water threshold (300 mg/L) but remained below most industrial limits 500 mg/L **[16]**. Elevated Cl^- and Na^+, however, may accelerate corrosion of metal installations. The corrosive Na–Cl water can equally impact underground installations **[16]**. Another parameter of interest was total hardness (TH). Total hardness (as $CaCO_3$) in the groundwater of the study area varied widely from 5 mg/L to 570 mg/L (Table 4). This reflected heterogeneity in rock–water interaction and mixing. Higher TH occurs where Ca/Mg inputs (from weathering or cation exchange) accumulate, and lower TH where fresh water recharge dilutes ions. Some samples (especially the inland well, LV) fell in the 61–120 mg/L range depicting moderately hard water, but others approached 500 mg/L (Table 4) and above. Similar results were obtained by **[9]** in a study on groundwater, where he observed that coastal groundwater was moderately hard, through hard to very hard. According to WHO, total hardness above 500 mg/L (as $CaCO_3$) is usually considered "aesthetically unacceptable".

The Limbe study found TH often exceeding 300 mg/L, meaning some of the wells produced very hard water. The water remained calcium/magnesium-rich throughout, consistent with continuous rock weathering and exchange reactions controlling the water chemistry.

WHO does not set health-based limits for TH, but recommended managing it for aesthetic and operational reasons.

Table 4: Total Hardness (CaCO3) classification by Sawyer and [58]

TH Range	Class	Water types observed in the study area
0–60 mg/L	Soft	Boreholes, LV (33.3%)
61–120 mg/L	Moderately hard	LV (66.7%)
121–180 mg/L	Hard	W7
>180 mg/L	Very hard	W6

Therefore, the implications on water quality for industrial purpose is that high TH can cause scaling on industrial installations. Equally, very low TH, as seen in boreholes, may promote corrosivity. It is therefore advisable for any company to take necessary precautions such as pretreatment strategies (ion exchange, desalination) or cathodic protection in order to protect corrosion of their installations.

4. CONCLUSION

The overall combined hydro-chemical evidence suggests incipient seawater intrusion into the shallow coastal aquifer of the study area, but the intrusion is still in an early/moderate stage.

Sodium and chloride were the dominant major ions and the cation abundance was in the order $Na^+ > Ca^{2+} > Mg^{2+} > K^+$ while the anion abundance was in the order $Cl^- > SO_4^{2-} > HCO_3^- > NO_3^-$. This gave a pattern said to be typical of coastal aquifers influenced by seawater. Major ions concentrations plotted on the Piper diagram indicated four main water facies; Na–Cl saline water type, Ca–Cl, Ca–Na–HCO_3^- mixed water type and Ca–HCO_3^- freshwater type in the monitoring wells while the boreholes exhibited three major types, Ca–Cl, Ca–Na–HCO_3^- and Ca–HCO_3. Well W6 was the most affected while the inland well, LV was more or less experiencing seawater influx during land submergence at high tides. However, key ionic ratios for instance, most Na/Cl >0.86, moderate Cl/HCO_3, and localized low SO_4 /Cl observed in the samples, implied mixing rather than wholesale replacement by seawater. The correlation matrix points to mixing of freshwater and seawater with some clay exchange. The EC–TDS–major-ion correlation cluster strongly points to progressive salinization from the sea while the classic geochemical effect of intrusion, where Na replaces Ca on exchange sites is consistent with the predominance

of Na–Cl facies. With high NO_3^- being a classic sign of land-derived pollution, the anti-correlation of NO_3^- with the seawater indicators points to anthropogenic inputs on fresher groundwater. Though the TDS in well, LV (mean 362 mg/L) and W6 (mean 282 mg/L) approached the soft- water threshold (300 mg/L) this remained below the 500 mg/L industrial limits. However, elevated Cl^- and Na^+ may accelerate corrosion of metal installations.

This study found out that some of the wells produced very hard water as TH often exceeded 300 mg/L in most of the samples. A proper groundwater management plan would be necessary and such should include measures to control the rate of water extraction, how to artificially recharge the aquifer and setting up of buffer- zones. From the study analysis, it can be observed that the groundwater is not suitable for industrial installations. It is recommended to take necessary precautions to protect industrial installations from scaling and corrosion through pretreatment strategies (ion exchange, desalination) or by protecting the cathodes.

Acknowledgements Special thanks go to the "Partners Enhancing Resilience to People Exposed to Risks Universities (PERIPERI U)" of the University of Buea (funded by USAID) for providing partial funding for the field work and laboratory analysis of the samples during this research work.

References:

[1] Sherif, M., Sefelnasr, A., Javadi, A. (2012). Incorporating the concept of equivalent freshwater head in successive horizontal simulations of seawater intrusion in the Nile Delta aquifer, Egypt, Journal of Hydrology 464-465, 186-198.

[2] Gopinath, S., Srinivasamoorthy, K., (2015). Application of Geophysical and hydrogeochemical tracers to investigate salinisation sources in Nagapatinam and Karaikal Coastal Aquifers, South India. Aquatic Procedia 4, 65–71.

[3] Singh, A. (2014). Groundwater resources management through the applications of simulation modeling: a review. Science of the Total Environment 499, 414-423.

[4] Masciopinto, C. (2006) Simulation of coastal groundwater remediation: The case of Nardò fractured aquifer in Southern Italy. Environ. Model. Softw., 21, 85–97.

[5] Mjemah, I. C., Van Camp, M., Walraevens, K. (2009) Groundwater exploitation and hydraulic parameter estimation for a Quaternary aquifer in Dar es Salaam Tanzania. J Afr Earth Sci 55:134–146

[6] Van Camp, M., Mtoni, Y. E., Mjemah, I. C., Bakundukize, C., Walraevens, K. (2014) Investigating seawater intrusion due to groundwater pumping with schematic model simulations: The example of the Dar Es Salaam coastal aquifer in Tanzania. J. Afr. Earth Sci., 96, 71–78.

[7] Ko, S. H., Ishida, K., Oo, Z. M., Sakai, H. (2021) Impacts of seawater intrusion on groundwater quality in Htantabin township of the deltaic region of southern Myanmar. Groundw. Sustain. Dev.14:100645.

[8] Vengosh, A., Kloppmann, W., Marei, A., Guerrot, C., Pankratov, I., Raanan, H. (2005) Sources of salinity and boron in the Gaza Strip: National contaminant flow in southern Mediterranean coastal aquifer. Water Resources Research, Vol. 41 W01013, doi:101029/2004WR003344.

[9] Akoachere, R. A., Etone, E. N., Mbua, R. L., Ngassam, M. P., Longonje, S. N., Oben, P. M. and Engome, R. W. (2019) Trace Metals in Groundwater of the South Eastern Piedmont Region of Mount Cameroon: Quantification and Health Risk Assessment. Open Access Library Journal, 6, e5327.

[10] Taylor, R. G., Scanlon B., Döll P. (2013a) Ground water and climate change. Nat Clim Change 3: 322–329.

[11] GWP/CAFTAC, 2010. Global Water Partenarship Central Africa. Cameroon Report pp.210.

[12] Werner, A. D., Bakker, M., Post, V. E. A., Vandenboede, A., Lu, C. H., Ataie-Ashtiani, B., Simmons, C. T., Barry, D. A. (2013) Seawater intrusion processes, investigation and management. Recent advances and futures challenges. Adv. Water Resources, 51, 3–26.

[13] Nair, I. S., Renganayaki, S. P., Elango, L. (2013) Identification of seawater intrusion by Cl/Br ratio and mitigation through managed aquifer recharge in aquifers North of Chennai India. J. Groundw. Res., 2: 155-162

[14] Esteller, M. V., Rodríguez, R., Cardona, A., Padilla-Sánche, L. (2012). Evaluation of hydrochemical changes due to intensive aquifer exploitation: case studies from Mexico. Journal of Environ. Monitoring and Assessment 9: 5725-5741.

[15] Motchemien, R. and Fonteh, M. F. (2020). The impact of sea water intrusion on the spatial variability of the physical and chemical properties of ground water in Limbe-Cameroon Afr. J. Environ Sci. Technol. 14(4), 92-103
[16] Asadollahfardi, G., Rezaei, M., & Azizi, R. (2016). Evaluation of groundwater quality for industrial uses in the Eslamshahr region, Iran. Environmental Earth Sciences, 75(4), 1-12.
[17] Bano, A., Begum, Z. A., Rahman, I. M., Hasegawa, H., & Sawai, H. (2017). Groundwater quality assessment for industrial use in Chittagong, Bangladesh: Importance of semi-quantitative risk appraisal. Journal of Cleaner Production, 156, 402-411.
[18] Lazarova, V., Sturny, V., & Sang, G. T. (2012). Relevance and benefits of urban water reuse in tourist areas. Water, 4(1), 107–122.
[19] Ngoran, A., Ako, A. A., Egbe, E. A., Suh, C. E., & Yongue-Fouateu, R. (2015). Hydrogeochemistry of groundwater in the Limbe area, Southwest Region, Cameroon. Journal of Geochemical Exploration, 156, 72-84.
[20] Jones, B. F., Vengosh, A., Rosenthal, E., Yechieli, Y. (1999). Geochemical investigation of groundwater quality. In Seawater Intrusion in Coastal Aquifers-Concepts, Methods and Practices; Springer: Kluwer, The Netherlands; pp. 51–71.
[21] National Institute of Statistics (NIS) (2013). Annual statistic of Cameroon, Yaoundé, Cameroun: INS.
[22] APHA. (2017). Standard methods for the examination of water and wastewater (23rd ed.). American Public Health Association.
[23] Dhakate, R. r., Venkata, R. G., Sankaran, S. (2020). Hydrogeochemical and isotopic study for assessment of saline water ingression into shallow coastal aquifers of Udupi District, Karnataka, India, Geochem. J. 80 (4) Article No. 125647.
[24] Appelo, C. A. J., & Postma, D. (2005). *Geochemistry, groundwater and pollution*. Taylor & Francis.
[25] Patel, P., Raju, N. J., Reddy, B. C. S. R., Suresh, U., Gossel, W., & Wycisk, P. (2016). Geochemical processes and multivariate statistical analysis for the assessment of groundwater quality in the Swarnamukhi River basin, Andhra Pradesh, India. Environmental Earth Sciences, 75(7), 1-24.
[26] Hounslow, A. (1995). Water quality data: analysis and interpretation. Boca Raton: CRC press.
[27] Utom, A. U., Odoh, B. I., & Egboka, B. C. (2013). Assessment of hydrogeochemical characteristics of groundwater quality in the vicinity of Okpara coal and Obwetti fireclay mines, near Enugu town, Nigeria. Applied Water Science, 3(1): 271-283.
[28] Piper, A. M. (1994) A graphical procedure in the chemical interpretation of groundwater analysis, Trans. Am. Geophys. Union 25, 914–923.
[29] World Health Organization (WHO) (2017). Guidelines for Drinking Water Quality, 4th ed.; incorporating the first addendum; World Health Organization: Geneva, Switzerland. https://apps.who.int/iris/bitstream/handle/10665/254637/9789241549950-eng. pdf?sequence=1
[30] Abdelkader, T., Ahmed and Ibrahim Askri (2014) Environmental characteristics of the ground water aquifer in a coastal area of Oman. Conference Paper: https://www.researchgate.net/publication/278404837
[31] Pulido-Bosch, A., Tahiri, A., Vallejos, A. (1999). Hydrogeochemical characteristics of processes in the Temara Aquifer in Northwestern Morocco. Water Air Soil Pollut., 114, 323–337.
[32] Walraevens, K., Van Camp, M. (2004) Advances in understanding natural groundwater quality controls in coastal aquifers. In Proceedings of the 18th Salt Water Intrusion Meeting (SWIM), Cartagena, Spain; pp. 451–460.
[33] Khan, A.F., Srinivasamoorthy, K., Prakash, R., Rabina, C. (2021). Hydrochemical and statistical techniques to decode groundwater geochemical interactions and saline water intrusion along the coastal regions of Tamil Nadu and Puducherry, India. Environ. Geochem. Health, 43, 1051–1067.
[34] Chadha, D. K. (1999) A proposed new diagram for geochemical classification of natural waters and interpretation of chemical data. Hydrogeol. https://doi.org/10.1007/s100400050216
[35] Mondal, N. C., Singh, V. P., Singh, V. S., Saxena, V. K. (2010) Determining the interaction between groundwater and salinewater through groundwater major ions chemistry. Journal of Hydrology, DOI: 10.1016/j.jhydrol.2010.04.032.
[36] Aladejana, J. A., Kalin, R. M., Sentenac, P., & Hassan, I. (2021). Groundwater quality index as a hydrochemical tool for monitoring saltwater intrusion into coastal freshwater aquifer of Eastern Dahomey Basin, Southwestern Nigeria. Groundwater for Sustainable Development, 13, 100568. https://doi.org/10.1016/j.gsd.2021.100568

[37] Telahigue, F., Souid, F., Agoubi, B., Chahlaoui, A., & Kharroubi, A. (2020). Hydrogeochemical and isotopic evidence of groundwater salinization in a coastal aquifer: A case study in Jerba Island, southeastern Tunisia. Physics and Chemistry of the Earth, Parts A/B/C, 118–119, 102886. https://doi.org/10.1016/j.pce.2020.102886
[38] Abdalla, F. (2015). Ionic ratios as tracers to assess seawater intrusion and to identify salinity sources in Jazan coastal aquifer, Saudi Arabia. Arabian Journal of Geosciences, 9(1), 40. https://doi.org/10.1007/s12517-015-2065-3
[39] Schoeller, H. (1956). Géoochimie des eaux souterraines application aux eaux des gisements de pétrole. Institut Français du Pétrole.
[40] Tran, D. A., Tsujimura, M., Vo, L. P., Nguyen, V. T., Kambuku, D., & Dang, T. D. (2020). Hydrogeochemical characteristics of a multi-layered coastal aquifer system in the Mekong Delta, Vietnam. Environmental Geochemistry and Health, 42(2), 661–680. DOI: 10.1007/s10653-019-00400-9
[41] Müller, D., Blum, A., Hart, A., Hookey, J., Kunkel, R., Scheidleder, A., Tomlin, C., Wendland, F. (2006) Final Proposal for a Method ology to Set up Groundwater Threshold Values in Europe. BRIDGE Deliverable D18. 63p.
[42] Singh, C. K., Shashtri, S., Mukherjee, S. (2010) Integrating multivariate statistical analysis with remote sensing and GIS for geochemical assessment of groundwater quality: a case study of Rupnagar districtin Shiwaliks of Punjab. India Earth Environ Sci. 62(7):1387–1405
[43] Thomas, C., Orban, P., Brouyère, S. (2016) Caractérisation de la Concentration de Référence de Certains Paramètres Chimiques Présents Naturellement dans les Masses d' eau Souterraine Captives du Socle et du Crétacé (BR01) et du Landénien (BR03) en Région de Bruxelles-Capitale; Bruxelles Environnement: Brussels, Belgium.
[44] Fidelibus, M. D., Balacco, G. Alfio, M. R. Arfaoui, M., Bassukas, D., Güler, C., Hamzaoui-Azaza, F., Külls, C., Panagopoulos, A., Parisi, A., Sachsamanoglou, E., Tziritis, E. (2025). A chloride threshold to identify the onset of seawater/saltwater intrusion and a novel categorization of groundwater in coastal aquifers, Journal of Hydrology, 653, 132775, ISSN 0022-1694 https://doi.org/10.1016/j.jhydrol.2025.132775.
[45] Vengosh, A., Spivack, A. J., Artzi, Y., Ayalon, A. (1999) Geochemical and boron, strontium and oxygen isotopic constraints on the origin of the salinity in groundwater from the Mediterranean coast of Israel, Water Resour. Res. 35 1877.
[46] Wang, H., Yang, Q., & Liang, J. (2022). Interpreting the salinization and hydrogeochemical characteristics of groundwater in Dongshan Island, China. Marine Pollution Bulletin, 178, 113634.
[47] Todd, D. K., & Mays, L. W. (2004). Groundwater Hydrology. John Wiley & Sons.
[48] Gao M, Sun Q, Dang X, Hou G, Guo F, Liu Z, Chang X and Zhao G (2023) Hydrogeochemical characteristic and recognization of saline groundwater formation and evolution in silty coast of the Yellow Sea and Bohai Sea, Eastern China. *Front. Earth Sci.* 11:1186661.
[49] Mercado, A. The use of hydrogeochemical patterns in carbonate sand and sandstone aquifers to identify intrusion and flushing of saline waters. Groundwater 1985, 23, 635–664.
[50] ElMoujabber, M., Bou Samra, B., Darwish, T., Atallah, T. (2006) Comparison of different indicators for groundwater contamination by seawater intrusion on the Lebanese coast. Water Resour. Manag. 20, 161–180.
[51] Abu-alnaeem, M., Yusoff, I., Ng, T., Alias, Y., May, R., & Haniffa, M. (2019). An integrated multi-techniques approach for hydrogeochemical evaluation of ion exchange processes and identification of water types based on statistical analysis: Application to the Gaza coastal aquifer, Gaza Strip, Palestine. Groundwater for Sustainable Development, 9, 100227.
[52] Prasanna, M. V., Chidambaram, S., & Srinivasamoorthy, K. (2010). Statistical analysis of the hydrogeochemical evolution of groundwater in hard and sedimentary aquifers system of Gadilam river basin, South India. Journal of King Saud University - Science, 22(3), 133–145.
[53] Srinivasamoorthy, K., Nanthakumar, C., Vasanthavigar, M., Vijayaraghavan, K., Rajivgandhi, R., Chidambaram, S., Anandhan, P., Manivannan, R., & Vasudevan, S. (2011). Groundwater quality assessment from a hard rock terrain, Salem district of Tamilnadu, India. Arabian Journal of Geosciences, 4(1), 91–102. https://doi.org/10.1007/s12517-009-0076-7
[54] Tay, C. K., Hayford, E, K., Hodgsoni, I. O. A. (2017). Application of multivariate statistical technique for hydrogeochemical assessment of groundwater within the Lower Pra Basin, Ghana. Appl Water Sci 7:1131– 11150.

[55] Mollema, P. N., Antonellini, M., Stuyfzand, P. J., Juhasz-Holterman, M. H. A., Van Diepenbeek, P. M. J. A. (2015) Metal accumulation in an artificially recharged gravel pit lake used for drinking water supply. J. Geochem. Explor. 2015, 150, 35–51.
[56] Nawal Alfarrah and Kristine Walraevens (2018) Groundwater Overexploitation and Seawater Intrusion in Coastal Areas of Arid and Semi-Arid Regions
[57] Stuyfzand, P. J. (1986) A new hydrogeochemical classification of water types: Principles and application to the coastal dunes aquifer system of the Netherlands. In Proceedings of the 9th SWIM, Delft, The Netherlands, 12–16 May pp. 641–656
[58] McCarthy, P. L., Sawyer, C. N. (1967). Chemistry for sanitary engineers, 2nd edition. McGraw-Hill, New York